# Ultra-wideband on-body elliptical monopole antenna

Duy Hai Nguyen,[1,✉] Viktor Krozer,[1] Jochen Moll,[1] and Gernot Zimmer[2]

[1] *Institute of Physics, Goethe University Frankfurt, Frankfurt am Main, Germany*

[2] *RF Engineering, Frankfurt University of Applied Sciences, Frankfurt am Main, Germany*

✉E-mail: nguyen@physik.uni-frankfurt.de

This study presents an ultra-wideband, elliptical slot, planar monopole antenna for early breast cancer microwave imaging. The on-body antenna's operation is optimised by direct contact with the patient's skin. With a compact size of 9 × 7 mm, the antenna covers a wide bandwidth from 16 to 24 GHz for reflection coefficients lower than –10 dB. Besides, it also features an electrode for electrical impedance tomography applications. Verification on a volunteer's breast gives an excellent agreement with the simulation for the defined bandwidth. Furthermore, as the first stage of the system's characterisation, pork fat is also used to demonstrate the possibility to enhance the transmission between the antennas within the high loss environment. Those results propose the feasibility of implementing a high-frequency radar system for breast cancer detection.

*Introduction:* Microwave imaging (MI) has emerged as a promising alternative or supplementary method for breast cancer diagnosis. In fact, instead of the ionising radiation, MI techniques produce low-risk results by investigating transmitting and scattering signals within the patients. Several kinds of research and experiments have been studied over the past decades to demonstrate the capabilities of breast cancer detection by using MI. A MI system, including 60 aperture slot, monopole elements, was introduced by Preece *et al*. [1]. The authors were able to acquire three-dimensional, reconstructed images from 86 patients by sweeping the operating frequency from 3 to 8 GHz. Similarly, other systems were also proposed [2–4]. In those systems, the maximum frequency is often limited to 10.3 GHz due to higher losses of the penetrating signals within the tissue. Hence, the resolution of the reconstructed images is limited due to the low operating frequency. There have been few studies, which investigate the feasibility of millimetre-wave detecting systems for higher resolution images. Recently, Di Meo *et al*. [5] demonstrated an experiment with rectangular waveguides, operating at 30 GHz, to detect cancerous tumours in *ex vivo* breast models. However, the results have not been verified by practical applications yet.

In this study, we propose an ultra-wideband (UWB), elliptical slot, planar monopole antenna for early breast cancer detection. The antenna's operating frequency range from 16 to 24 GHz compromises a better-reconstructed image quality (higher resolution) and high-dynamic-range hardware requirements due to the significant signal attenuation in the tissue at these frequencies. Furthermore, an additional aperture on top of the antenna is optimised to be suitable for electrical impedance tomography (EIT) studies. Hence, a multi-functional antenna structure is obtained.

*Antenna design:* A stack of RO4350B laminates [6] is used for the antenna's design as shown in Figure 1. Thanks to the multi-layer technology, the antenna, and its excitation network are integrated into the same structure. A ground plane (i.e., L3 layer) also improves isolation between the radiating and other elements [7]. The substrate thickness for the antenna and the feeding network, respectively, is $h_{antenna} = 0.95$ mm and $h_{feed} = 0.25$ mm. Here, a coaxial probe is used to transmit excitation power from the bottom layer to the radiating patch. Regarding Figure 1, a back-cavity is also implemented by via holes. Usages of via holes exhibit the advantages of reducing the overall design's dimension, increasing the integration capability of different components, and improving microwave characteristics of the structure.

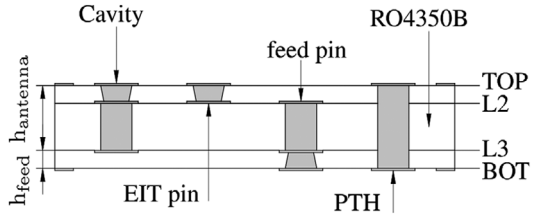


**Fig. 1** *Schematic of a multi-layer structure of the antenna*

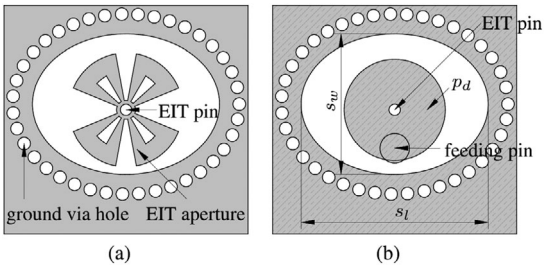


**Fig. 2** *Schematic of the antenna structure. (a) Top layer: Electrical impedance tomography aperture. (b) L2 layer: Ultra-wideband monopole antenna*

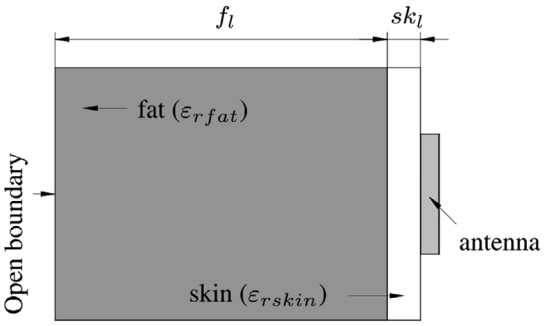


**Fig. 3** *Simulation setup for an on-body antenna*

*Elliptical slot monopole antenna:* In our work, a microstrip monopole antenna is used, which is commonly adopted for UWB microwave tomography systems. Instead of broadside radiation, the directivity of the antenna is improved by using an elliptical slot with a back-cavity as shown in Figure 2(b). Due to the dielectric properties of the breast tissue, it has been shown that higher frequency signals suffer significant attenuation when propagating within the breast [1]. For this reason, the antenna's characteristics and radiating power are preserved by placing the main circular radiator at the L2 layer, which is not in contact with the skin. Regarding Figure 2(b), major and minor axes of the slot are $s_l = 7.4$ mm and $s_w = 4.6$ mm, respectively, and the patch has a diameter of $p_d = 4$ mm. In addition, the back-cavity (ground via hole) helps to improve the antenna characteristics by short-circuiting surface waves propagation into the ground [8]. On the other hand, an electrode, namely, EIT aperture, for EIT [9] is placed on top of the antenna. Here, we optimise the aperture's shape to achieve a maximum area for the EIT applications while retaining minimum impact on the antenna's radiation.

*Simulation conditions:* Figure 3 shows a simple simulation setup to optimise the antenna's performance when it directly contacts the patient's skin. Here, a compressed breast structure is simplified by a stack of homogeneous skin and fat layers. Open boundaries are applied to the breast models to prevent any reflection. In this work, dielectric properties of the female breast (e.g., skin, fat, and cancerous tissue) are developed based on the Cole–Cole equivalent models from the *ex vivo* breast tissue [10]. Figure 4 represents the real ($\varepsilon'$) and imaginary parts ($\varepsilon''$) of the dielectric constants for the breast models in the simulation.

*Measurements:* A 2 × 2 antenna array prototype, as shown in Figure 5, is realised and verified by a vector network analyser (VNA). Maximum

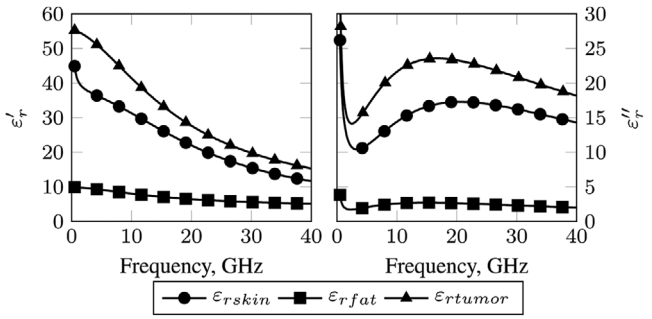


**Fig. 4** *Dielectric properties of the breast tissue in the simulation*

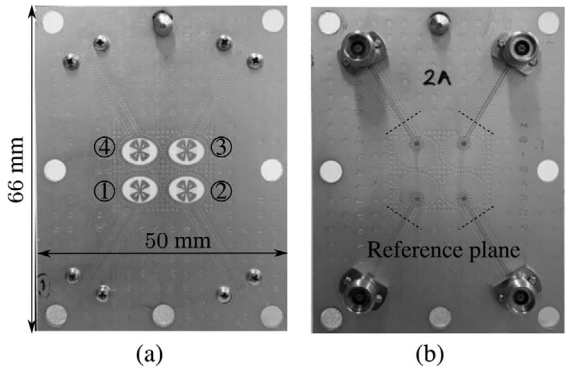


**Fig. 5** *Photographs of the antenna prototype. (a) Top. (b) Bottom*

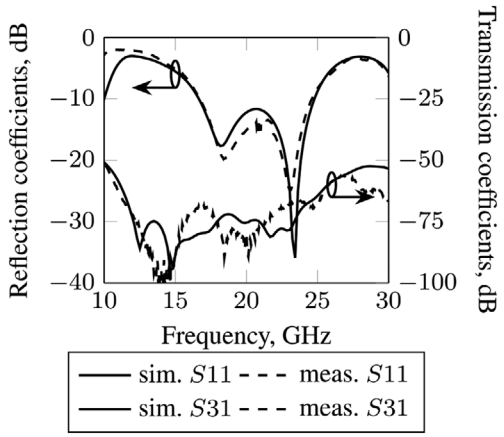


**Fig. 6** *S-parameters measurement results of the antenna elements 1 and 3, conducted on a female volunteer*

excitation output power from the VNA is –15 dBm with a dynamic range of approximately 90 dB. The measured results are recorded and computed by the multi-line TRL (thru-reflect-line) calibration [11] to have the same reference planes as the simulation (Figure 5(b)). We conducted two different measurements on a female volunteer and pork fat, respectively, to characterise the antenna.

*Measurements on a female volunteer:* A measurement procedure with a female volunteer is described as follows:

1. Characteristics of a single antenna: The volunteer is asked to keep the antenna array (Figure 5) well contacted with her skin, and the *s*-parameters are recorded. For example, the measured results of the antenna pair 1–3 are shown in Figure 6. The measured reflection coefficients at the antenna input show an excellent agreement with the simulation. A practical bandwidth is 7.9 GHz (from 16.7 to 24.6 GHz) for the reflection coefficients to be lower than –10 dB. On the other hand, the transmission coefficients (i.e., mutual couplings in this case) between the elements 1–3 also match well with the calculation.

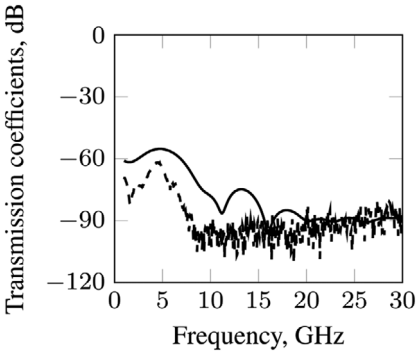


**Fig. 7** *Transmission coefficients between simulation and measurement of the direct opposite antenna elements, conducted on a compressed breast of 30 mm*

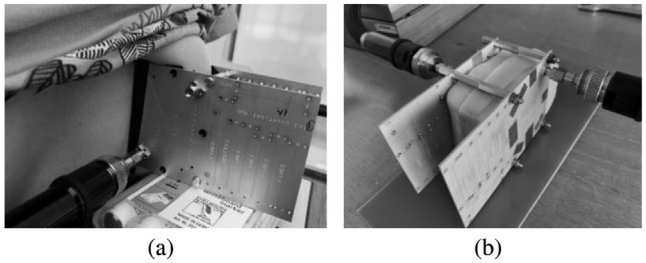


**Fig. 8** *Photographs of simple measurement setups for the detection scenario. (a) With female breast. (b) With pork fat*

2. Transmission within a compressed breast: In the next step, the breast is compressed to a thickness of 30 mm by two parallel arrays as illustrated in Figure 8(a). Figure 7 shows the measured transmission coefficients from the direct opposite antenna elements. According to the results, the VNA can capture the low power signals up to 9 GHz. Beyond this frequency, the transmitted power level is below the noise floor of the equipment. However, the results show a good similarity between the measurement and calculation. The measured values are approximately 10 dB lower than those calculated, which could be explained by two reasons:
   i. The mechanical stability is not sufficient to properly compress the breast. As a result, the antennas are practically misaligned, and there is an air gap between the breast and the antennas. These factors increase the power losses of the signal transmission.
   ii. The Cole–Cole equivalent models of the breast tissue are the average values of the *ex vivo* measurements. Therefore, there is a lack of information about the patient's age from mathematical models. In addition, compared to the models, the measured results are obtained by the *in vivo* measuring conditions. Finally, the simple breast tissue (Figure 3) was used to reduce simulation time, which represents a trade-off between simulation speed and accuracy of results. However, the chosen simplified tissue models still accurately represent the measured results.

*Measurements on a pork fat sample:* We also use pork fat to evaluate the transmission capabilities of the antennas in the tissue. As shown in Figure 8(b), a stack of several pork fat layers is compressed to a thickness of 40 mm, and a similar measurement process as in the previous section is made. Due to the geometry's symmetry, we can excite only one antenna on an array from one side (e.g. A1:1) and measure the receiving signals at four antennas on another array from the other side (e.g. A2). According to the results in Figure 9, distinguished complex transmission coefficients between different antenna pairs are suitable for further post-processing procedures. The detectable frequency is up to 25 GHz, which shows that the power significantly drops at the skin interfaces for the measurements with a female volunteer.

*Discussion:* We summarise some important points for the antenna design and its performance as follows:

*Table 1. Comparison of antenna designs for breast cancer microwave imaging*

| | $f_0$ (GHz) | BW (GHz) | Coupling medium | Antenna type | Material ($\varepsilon_r$) | Other features |
|---|---|---|---|---|---|---|
| This work | 20.65 | 7.9 | None | Monopole | 3.66 | Electrical impedance tomography |
| [1] | 5.5 | 4.95 | Water | Monopole | 10.2 | None |
| [2] | 3 | 2 | None | Monopole | 3.5 (flexible) | None |
| [4] | 5.6 | 6.72 | None | Monopole | 10.2 | None |
| [12] | 6.5 | 5 | None | Patch | 10.2 | None |

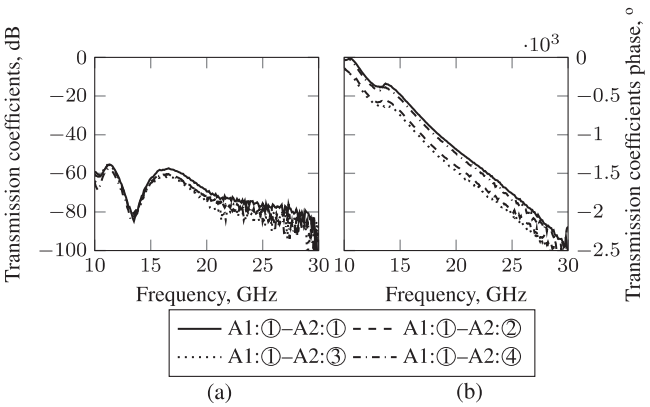


**Fig. 9** *Measured complex transmission coefficients between the transmitter A1:1 and the other four receivers in the array A2 with pork fat, compression of 40 mm. (a) Transmission coefficients. (b) Phases*

1. The antenna's design relies on a UWB, elliptical slot, microstrip monopole antenna. The measured bandwidth is from 16.7 to 24.6 GHz (return loss RL $\geq$ 10 dB). Common material RO4350B is used for the design.
2. The *ex vivo* Cole–Cole mathematical models for the breast tissue are suitable to predict the microwave performance within the breast. To enhance the accuracy of the models, empirical adjustments might be needed. In addition, a complex multi-layer structure of the breast tissue could also be used.
3. The dynamic range of the measurement setup can be improved with a low-noise receiver employing a low-noise amplifier at the VNA's input. Furthermore, higher excitation power signals could be applied, 0 dBm for example.
4. The experimental results from the pork fat suggest that the signals are mainly attenuated at the skin interfaces.
5. Table 1 compares the antenna in this work and other previous structures for breast cancer MI. The compared structures were also designed by planar technology, and verified by clinical tests. According to the table, our proposed antenna shows the major advantages of using low-cost material with an additional feature for EIT measurement.
6. Evaluation of the EIT feature is conducted by using a saline mixture (6.2 g/l). Measured conductivity of the solution is 80.8 S/m, while the referenced value is 90 S/m.

*Conclusion:* This study represents an antenna design method for early breast cancer detection using MI technique. Here, we develop an elliptical slot, microstrip monopole antenna to cover wide-bandwidth requirements. The measured impedance bandwidth is from 16.7 to 24.6 GHz for a reflection coefficient lower than –10 dB without a coupling medium. Also, the radiation directivity is enhanced by integrating a back-cavity via holes into the antenna's laminate. Despite using low-cost, low-dielectric constant material, the antenna still maintains a compact size, lightweight with expected performance. First measurements with a female volunteer and pork fat indicate the possibility to enhance signal transmission and thus to overcome the significant signal attenuation at high frequencies for a high-resolution microwave breast imaging system.

*Acknowledgement:* This work has been supported by the project IndiThera (13GW0361D) through the Federal Ministry of Education and Research (BMBF).

Open access funding enabled and organized by Projekt DEAL.



doi: 10.1049/ell2.12085

## REFERENCES

1 Preece, W., et al.: MARIA M4: Clinical evaluation of a prototype ultrawideband radar scanner for breast cancer detection. *J. Med. Imaging* **3**(3), 1–7 (2016)
2 Bahramiabarghouei, H., et al.: Flexible 16 antenna array for microwave breast cancer detection. *IEEE Trans. Biomed. Eng.* **62**(10), 2516–2525 (2015)
3 Norouzzadeh, E., et al.: Numerical and experimental analysis of a transmission-based breast imaging system: a study of application to patients. *Int. J. Microwave Wireless Technolog.* **12**(6), 469–476 (2020)
4 Hang, S., et al.: Detectability of breast tumor by a hand-held impulse radar detector: Performance evaluation and pilot clinical study. *Sci. Rep.* **7**(3), 1–11 (2017)
5 Di Meo, S., et al.: On the feasibility of breast cancer imaging systems at millimeter-waves frequencies. *IEEE Trans. Microwave Theory Tech.* **65**(5), 1795–1806 (2017)
6 *RO4000® High Frequency Circuit Materials*. Rogers Corporation, Chandler, Arizona (2017)
7 Balanis, C.: *Antenna Theory: Analysis and Design*. John Wiley & Sons, Hoboken, NJ (2005)
8 Nguyen, D.H., et al.: Improved sidelobe-suppression microstrip patch antenna array by uniform feeding networks. *IEEE Trans. Antennas Propag.* **68**(11), 7339–7347 (2020)
9 Oh, T.I., et al.: Validation of a multi-frequency electrical impedance tomography (mfEIT) system KHU Mark1: Impedance spectroscopy and time-difference imaging. *Physiol. Meas.* **29**(3), 295–307 (2008)
10 Martellosio, A., et al.: Dielectric properties characterization from 0.5 to 50 ghz of breast cancer tissues. *IEEE Trans. Microwave Theory Tech.* **65**(3), 998–1011 (2017)
11 Williams, D.F., Wang, C.M., Arz, U.: An optimal multiline trl calibration algorithm. In: IEEE MTT-S International Microwave Symposium Digest, Philadelphia, Pennsylvania, pp. 1819–1822 (2003)
12 Kuwahara, Y., et al.: Clinical test of microwave mammography. In: 2013 IEEE Antennas and Propagation Society International Symposium (APSURSI), Orlando, FL, pp. 2028–2029 (2013)